Journal of Rock Mechanics and Geotechnical Engineering xxx (xxxx) xxx

Contents lists available at ScienceDirect

Journal of Rock Mechanics and Geotechnical Engineering

journal homepage: www.jrmge.cn

Full Length Article

Deformation and damage properties of rock-like materials subjected to multi-level loading-unloading cycles

Zhizhen Liu [a,b,c], Ping Cao [b], Qingxiong Zhao [b], Rihong Cao [b], Fei Wang [a,b,*]

[a] Yellow River Laboratory, Zhengzhou University, Zhengzhou, 450001, China
[b] School of Resource and Safety Engineering, Central South University, Changsha, 410083, China
[c] School of Engineering, University of Warwick, Coventry, CV4 7AL, UK

ARTICLE INFO

Article history:
Received 20 June 2022
Received in revised form
9 September 2022
Accepted 14 November 2022
Available online xxx

Keywords:
Incremental cyclic loading-unloading
Unloading rate
Strain characteristics
Energy evolution
Damage model

ABSTRACT

In the process of engineering construction such as tunnels and slopes, rock mass is frequently subjected to multiple levels of loading and unloading, while previous research ignores the impact of unloading rate on the stability of rock mass. A number of uniaxial multi-level cyclic loading-unloading experiments were conducted to better understand the effect of unloading rate on the deformation behavior, energy evolution, and damage properties of rock-like material. The experimental results demonstrated that the unloading rate and relative cyclic number clearly influence the deformation behavior and energy evolution of rock-like samples. In particular, as the relative cyclic number rises, the total strain and reversible strain both increase linearly, while the total energy density, elastic energy density, and dissipated energy density all rise nonlinearly. In contrast, the irreversible strain first decreases quickly, then stabilizes, and finally rises slowly. As the unloading rate increases, the total strain and reversible strain both increase, while the irreversible strain decreases. The dissipated energy damage was examined in light of the aforementioned experimental findings. The accuracy of the proposed damage model, which takes into account the impact of the unloading rate and relative cyclic number, is then confirmed by examining the consistency between the model predicted and the experimental results. The proposed damage model will make it easier to foresee how the multi-level loading-unloading cycles will affect the rock-like materials.

1. Introduction

In the course of engineering construction, rocks are frequently subjected to cyclic loading and unloading, such as during the excavation of underground caverns and reinforcement of steep slopes. The equilibrium state of in situ stress will change as a result of the excavation of underground chambers, which include the tunnel, roadway, and storage, resulting in cyclic loading and unloading of the surrounding rock (Yang and Hu, 2018; Peng et al., 2019; Duan et al., 2020; Hu et al., 2020a). Numerous studies have demonstrated that when rock mass is subjected to cyclic loading and unloading, its mechanical properties are very different from those under monotonic static loading (Momeni et al., 2015; Pouya et al., 2016; Vaneghi et al., 2020a; Zhang et al., 2020, 2021; Zhou et al., 2020; Shirani Faradonbeh et al., 2021; Wang et al., 2021). In comparison to monotonic loading, cyclic loading-unloading of rock materials is much more likely to damage and fail the rock mass (Bagde and Petroš, 2005; Vaneghi et al., 2018; Chen et al., 2019).

Engineering rock masses frequently experience a type of load known as constant amplitude cyclic loading. The majority of current research focuses on how cyclic loading parameters affect the mechanical behavior and damage of rock mass. The studied loading parameters mainly include the waveform (Taheri et al., 2016), amplitude (Vaneghi et al., 2020b; Wang et al., 2020; Zhu et al., 2021), frequency (Li et al., 2020), stress level (Chen et al., 2020), number of cycles (Chen et al., 2017), loading rate (Huang and Li, 2014; Meng et al., 2016, 2019; Zhang et al., 2018). In particular, the effect of waveforms, i.e. triangular, sinusoidal, and square, on the damage response of rock was investigated. The results showed that the cumulative fatigue damage of rock impacted by a cyclic loading of a sine waveform is worse than that of a square waveform, but better than that of a triangular waveform (Xiao et al., 2008).

* Corresponding author. Yellow River Laboratory, Zhengzhou University, Zhengzhou, 450001, China.
E-mail address: wangfei0826@163.com (F. Wang).

Peer review under responsibility of Institute of Rock and Soil Mechanics, Chinese Academy of Sciences.

https://doi.org/10.1016/j.jrmge.2022.11.009

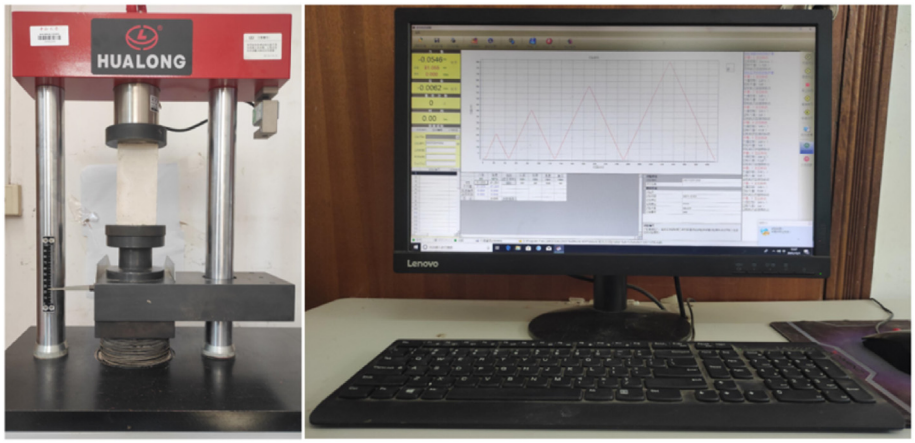

Fig. 1. The WHY-300/10 microcomputer servo-controlled pressure test machine.

With the increase of loading amplitude, the fatigue life becomes shorter, and the strength degradation and total strain increase (Ma et al., 2013). The compressive strength and total strain will decrease with an increase in loading frequency (Ma et al., 2013), as will fatigue (Pouya et al., 2016) and energy release (Bagde and Petroš, 2009). And the level of cyclic stress is positively correlated with the strength damage of rock (Ma et al., 2013). The elastic modulus and compressive strength of salt rock also decrease as the number of cycles increases (Fuenkajorn and Phueakphum, 2010). The loading rate also obviously affects the damage level of the rock mass. The damage generated inside the rock increases with the loading rate for a given amount of time (Lavrov, 2001). These results showed that the fatigue, damage, and failure behaviors of rock materials are significantly influenced by cyclic loading parameters.

In fact, in engineering practice, cyclic stresses are not always of constant amplitude (Peng et al., 2020; Zhou et al., 2020; Wang et al., 2021). For instance, the cyclic load created by the rise and fall of the water level in a hydropower plant is multi-level; in underground mining, the cyclic load created by blasting also acts on a certain structure in a multi-level form (Jiang et al., 2017; Peng et al., 2020). Additionally, the process of gas injection and production in the gas storage involves cyclic loading-unloading with stresses of various amplitudes, which may be equivalent to multi-level cyclic loading-unloading (Liu et al., 2014). In light of the aforementioned engineering issues, research results indicated that multi-level cyclic loading-unloading is more likely to result in instability and failure of the excavated rock mass than constant amplitude cyclic loading-unloading (Heap and Faulkner, 2008; Heap et al., 2009; Kendrick et al., 2013; Jia et al., 2018). Additionally, the deformation behavior of rocks subjected to multi-level cyclic loading-unloading is significantly different from that under constant amplitude cyclic loading-unloading (Jia et al., 2018).

The majority of earlier studies have, to this point, made an effort to assess how constant amplitude cyclic loading affects the mechanical characteristics of rocks. However, the mechanical characteristics, energy evolution and damage behaviors of rock materials subjected to multi-level cyclic loading-unloading were rarely studied. In addition, the impact of the unloading rate on the mechanical performance and damage behavior was overlooked. It is well known that the failure of rocks is essentially driven by energy (Meng et al., 2016, 2019; Wang et al., 2020; Zhou et al., 2022). Consequently, from the perspective of energy, it is of great practical significance to systematically investigate the effect of unloading rate on the mechanical behavior and energy evolution of rock materials subjected to multi-level loading-unloading cycles.

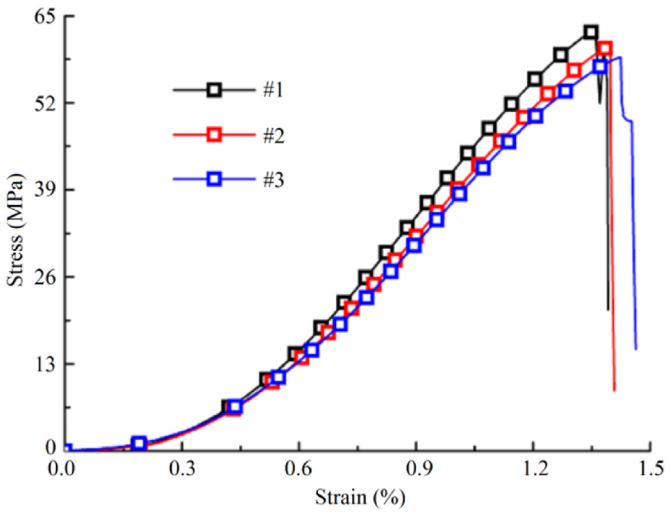

Fig. 2. The stress–strain curves of rock-like samples subjected to the monotonic static loading.

2. Experimental set-up

2.1. Experimental equipment

Through a WHY-300/10 microcomputer servo-controlled pressure test machine with a load capacity of 300 kN, the multi-level loading-unloading cycle tests were carried out at room temperature (25 °C). A computer system and a loading system make up the test system. Force control and displacement control are the two load control modes available for the test device. In the present test, the force control mode was chosen. The loading rate range is 0.015–15 kN/s. The test device is displayed in Fig. 1.

2.2. Experimental materials

Rock-like materials are widely used to study the mechanical behavior of rock mass, because they are not only affordable and simple to obtain, but also accurately reflect the mechanical characteristics of natural rock (Hu et al., 2019). In this study, we also used the rock-like sample to investigate the effect of the unloading rate on deformation behavior and energy evolution of rock. The 2:1:1 vol ratio of cement, sand, and water used to create the rock-like materials is a good representation of the mechanical properties

Please cite this article as: Liu Z et al., Deformation and damage properties of rock-like materials subjected to multi-level loading-unloading cycles, Journal of Rock Mechanics and Geotechnical Engineering, https://doi.org/10.1016/j.jrmge.2022.11.009

of sandstone (Lin et al., 2020, 2021a; Liu et al., 2022). According to the recommendations of previous research (Feng et al., 2019; Hu et al., 2020b; Lin et al., 2021b), the aspect ratio of the sample should be between 1 and 2 in order to effectively lessen the influence of the end effect on the test results. The sample was intended to be 30 mm thick, which can prevent both fracture failure from being too thin and irregular failure from being too thick along the thickness direction. According to earlier research (Hu et al., 2020b; Lin et al., 2021b), the dimensions of rock-like samples were 140 mm × 70 mm × 30 mm. The rock-like samples were kept in the curing box for 28 d at a temperature of 20 °C and a humidity of 95% before the mechanical test. Uniaxial compression tests with a loading rate of 0.5 kN/s were then performed on three rock-like samples. The stress–strain curves of the rock-like samples are shown in Fig. 2, It can be found from the figure that the deformation and strength properties of the rock-like samples have good consistency, and the average elastic modulus and average uniaxial compressive strength (UCS) of the samples are 6.2 GPa and 60.1 MPa, respectively. The stress–strain curves of the rock-like samples can be divided into four stages: initial compaction stage, linear elastic deformation stage, plastic deformation stage, and post-peak stage. The stress–strain curves of the rock-like samples (Fig. 2) are highly similar to that of sandstone reported by the previous findings (Meng et al., 2016, 2022; Vaneghi et al., 2018). As a result, the mechanical properties of rock-like samples can more accurately represent those of sandstone.

2.3. Experimental methodology

The initial load of the multi-level loading-unloading cycles is always set to 1 kN in order to prevent separation between the machine pressure plate and the sample during testing. The incremental loading gradient was set to 10 kN based on the rock-like sample's UCS. The maximum load is 11 kN for the first loading-unloading cycle, and 21 kN for the second loading-unloading cycle, as shown in Fig. 3a. The loading rate was fixed at 0.5 kN/s during the test, and the unloading rate ranged from 0.1 kN/s to 0.9 kN/s with a gradient of 0.2 kN/s. A total of five groups of multi-level loading-unloading cycle experiments were conducted, and three samples were include in each group. The loading and unloading continued until the rock-like samples were destroyed.

3. Calculation method of energy density

Energy is the primary cause of material deformation and damage (Meng et al., 2016, 2019; Wang et al., 2020). The energy absorption and dissipation can be viewed as a reflection of the structural change, including the compaction of original flaws, and the generation, propagation, and coalescence of new cracks, as well as the ultimate failure. Therefore, by studying the energy evolution, the deformation and damage mechanisms of rock-like materials can be discovered. The energy theory is predicated on the notion that there will not be any heat exchange between the tested rock-like sample and the environment outside (Feng et al., 2021). The total energy of rock-like samples from external loads can be divided into elastic and dissipated energy. Elastic energy is stored in rock, and dissipated energy is used to drive rock-like samples to generate irreversible deformation. Fig. 3b illustrates the calculation method for the elastic and dissipated energy densities of a single cyclic loading-unloading. The elastic and dissipated energy densities of rock-like materials in a loading- unloading cycle can be expressed as

$$\left.\begin{aligned} u_{\mathrm{p}} &= \frac{1}{2}\left[\int_{\varepsilon_0}^{\varepsilon_2}(\sigma_{\mathrm{li+1}}+\sigma_{\mathrm{li}})\mathrm{d}\varepsilon-\int_{\varepsilon_1}^{\varepsilon_2}(\sigma_{\mathrm{ui+1}}+\sigma_{\mathrm{ui}})\mathrm{d}\varepsilon\right] \\ u_{\mathrm{e}} &= \frac{1}{2}\int_{\varepsilon_1}^{\varepsilon_2}(\sigma_{\mathrm{ui+1}}+\sigma_{\mathrm{ui}})\mathrm{d}\varepsilon \end{aligned}\right\} \tag{1}$$

where u_{p} and u_{e} represent the dissipated and elastic energy densities, respectively; ε_0, ε_1 and ε_2 represent the strain at the initial loading point, the strain at the end point of unloading, and the strain corresponding to the upper stress σ_{u}, respectively; and σ_{l} is the lower stress.

The total elastic energy density and total dissipated energy density in multi-level loading-unloading cycles are calculated as

$$\left.\begin{aligned} U_{\mathrm{p}} &= \sum_{i=1}^{N}|u_{\mathrm{p}}|_i \\ U_{\mathrm{e}} &= \sum_{i=1}^{N}|u_{\mathrm{e}}|_i \end{aligned}\right\} \tag{2}$$

where U_{p} and U_{e} denote the total dissipated energy density and total elastic energy density in the multi-level loading-unloading cycles, respectively; and i and N represent the ith incremental cycle and the total cyclic number, respectively.

The total energy density of the rock-like sampleis the sum of the elastic and dissipated energy densities:

$$U = U_{\mathrm{p}} + U_{\mathrm{e}} \tag{3}$$

where U is the total energy density of rock-like sample in the multi-level loading-unloading cycles.

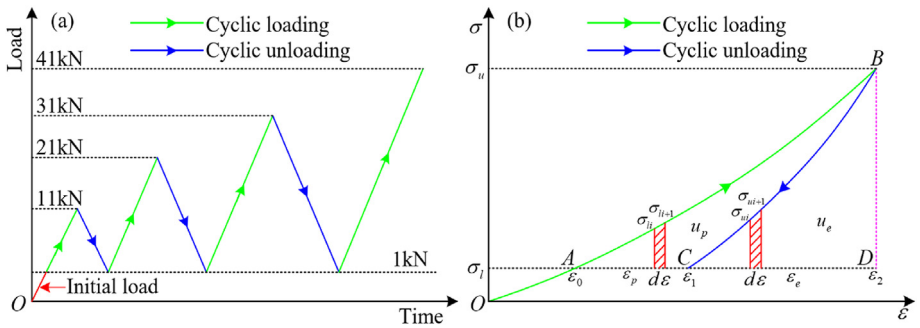

Fig. 3. (a) Schematic diagram of multi-level loading-unloading cycle path; and (b) Calculation principle of energy densities. ε_{p} and ε_{e} are the irreversible and reversible strains, respectively. The total strain is the sum of ε_{p} and ε_{e}.

Please cite this article as: Liu Z et al., Deformation and damage properties of rock-like materials subjected to multi-level loading-unloading cycles, Journal of Rock Mechanics and Geotechnical Engineering, https://doi.org/10.1016/j.jrmge.2022.11.009

4. Experimental results

4.1. Stress–strain curves

Fig. 4 displays the stress–strain curves of rock-like samples subjected to multi-level loading-unloading cycles. The peak stress of rock-like samples under the multi-level loading- unloading cycles is reduced by 13.3%–14.6% compared to that under monotonic static loading, suggesting that the sample may sustain damage as a result of the loading-unloading cycles. Additionally, Fig. 4 demonstrates that the stress–strain curve of the sample is relatively dense at the initial stage of cyclic loading-unloading and that the hysteresis loop is not immediately apparent. As it enters the later stage of cyclic loading-unloading, the stress–strain curve of the sample is relatively scattered, and forms a clear hysteresis loop. Additionally, the stress–strain curve of the sample shows that the unloading rate clearly affects the deformation and strength of rock-like samples. In particular, as the unloading rate increases, the stress–strain curve of the sample becomes denser at the initial stage of cyclic loading, indicating that the damage produced inside the sample decreases. Moreover, the strain that corresponds to the peak stress first falls and then rises, reaching a minimum value of 0.0119 at 0.5 kN/s. The peak strength of the sample also changed slightly from 51.3 MPa to 52.1 MPa as the unloading rate changed from 0.1 kN/s to 0.9 kN/s.

4.2. Strain characteristics

The relationship between strain parameters and the relative cyclic number under different unloading rates is depicted in Fig. 5. Fig. 5a illustrates that the total strain rises nearly linearly as the relative cyclic number rises. Additionally, the total strain also increases with the increase of unloading rate. The variation trend of reversible strain is very similar to that of total strain under the same unloading rate, as shown in Fig. 5b. The irreversible strain decreases with increasing unloading rate under the same relative cyclic number. The aforementioned experimental results are related to the frictional energy dissipation of microcracks during the unloading process. Microscopically speaking, loading causes the sample's microcracks to close, whereas unloading causes the compacted microcracks to reopen. Meantime, as elastic deformation from the sample's skeleton and particles is recovered, the larger unloading rate causes the recovery time of microcracks to be shorter, the recovery amount of microcracks becomes smaller, and the friction dissipation energy of microcracks gets smaller. The sample also has more elastic energy when less energy is dissipated

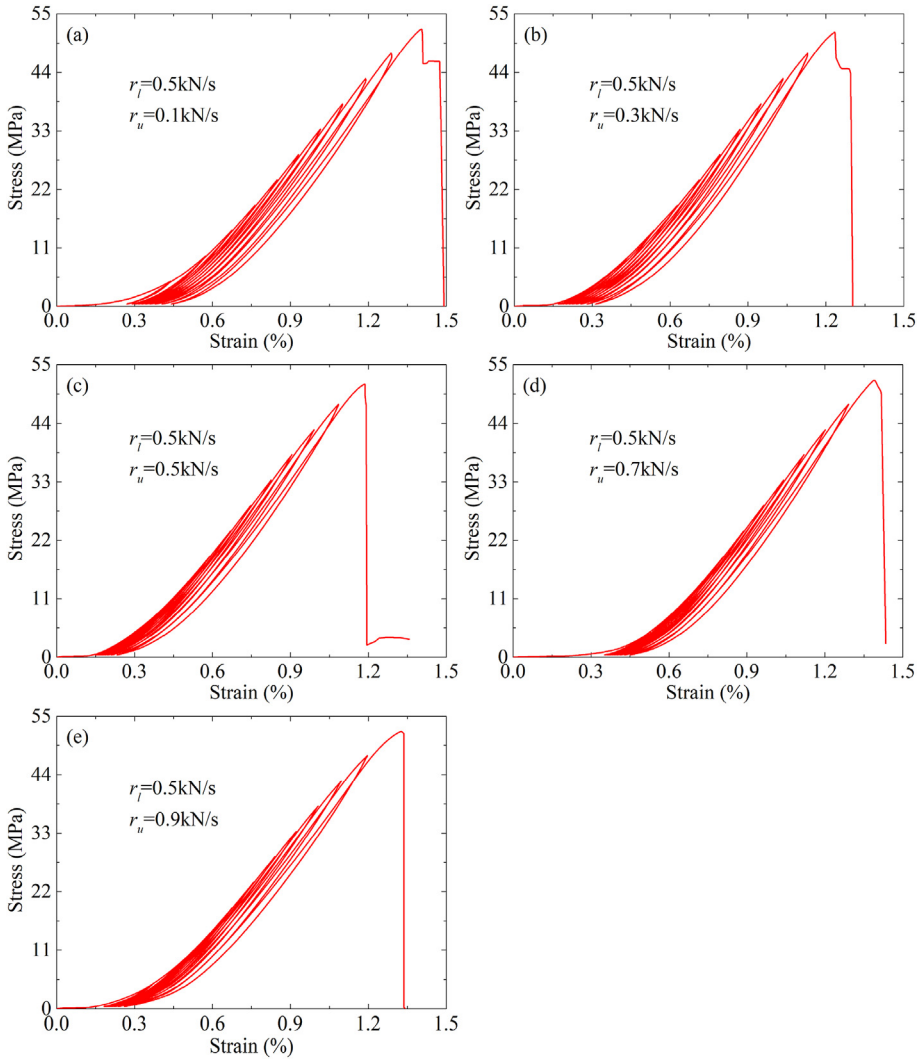

Fig. 4. The strain–stress curves of rock-like materials for different unloading rates. r_l is the loading rate, and r_u is the unloading rate.

Please cite this article as: Liu Z et al., Deformation and damage properties of rock-like materials subjected to multi-level loading-unloading cycles, Journal of Rock Mechanics and Geotechnical Engineering, https://doi.org/10.1016/j.jrmge.2022.11.009

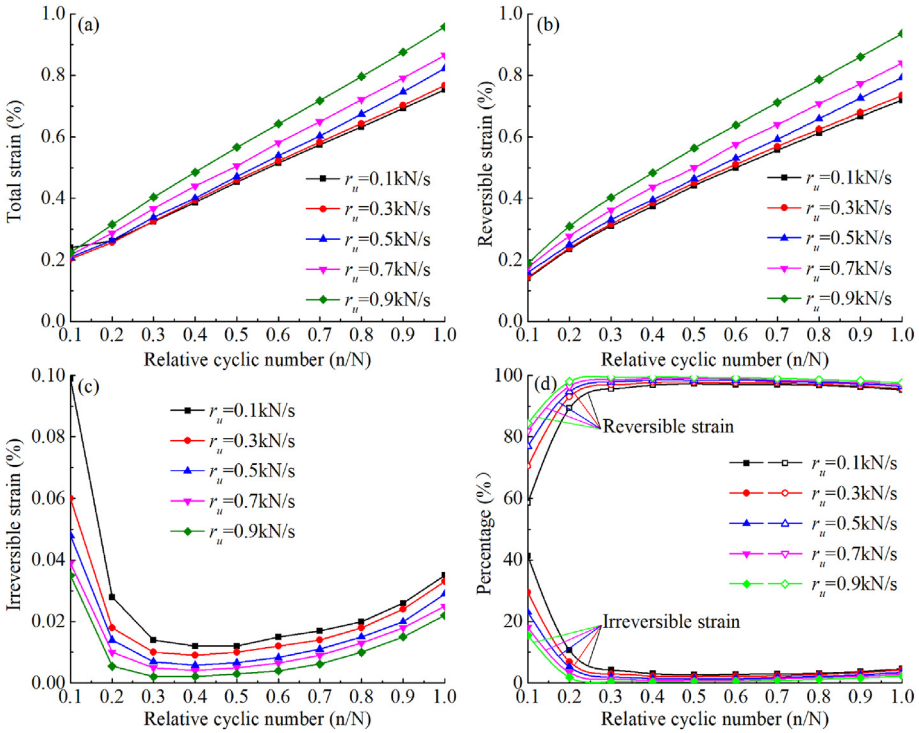

Fig. 5. Deformation law of rock-like materials with relative cyclic numbers under different unloading rates: (a) Total strain; (b) Reversible strain; (c) Irreversible strain; and (d) Percentage of reversible and irreversible strains in the total strain.

inside it. Therefore, the reversible strain increases and the irreversible strain decreases as the unloading rate increases.

The variation trend of the irreversible strain (Fig. 5c) is completely different from that of the total strain and reversible strain. The variation trend of the irreversible strain can be divided into three stages: rapid decline stage, steady stage and slow increase stage. The irreversible strain rapidly decreases when the relative cyclic number is less than 0.3. When the relative cyclic number is between 0.3 and 0.7, the irreversible strain is stable. The irreversible strain gradually increases when the relative cyclic number is greater than 0.7. In the initial loading-unloading cycle stage, the rapid decline of irreversible strain may be due to the compression and closure of the initial microscopic pores inside the samples.

The evolution trend of the percentage of reversible and irreversible strains is depicted in Fig. 5d. Fast increase, relative stability, and slight decrease stages are all included in the percentage curves of the reversible strain, whereas fast decrease, relative stability, and slight increase stages are all included in the percentage curves of the irreversible strain. Specifically, the percentage of reversible strain rises quickly and the percentage of irreversible strain falls precipitously when the relative cyclic number is between 0.1 and 0.3. The percentages of irreversible and reversible strains are essentially unchanged when the relative cyclic number is between 0.3 and 0.7. The percentage of reversible strain decreases slightly and the percentage of irreversible strain increases slightly when the relative cyclic number is between 0.7 and 1. It is important to note that at the stable stage, the reversible strain makes up nearly 95% of the total strain, which is 19 times more than the irreversible strain.

4.3. Energy density evolution characteristics

The total energy density, elastic energy density and dissipated energy density were calculated using Eqs. (1)–(3). The evolution of various energy density parameters of rock-like samples under various unloading rates is depicted in Fig. 6. The total energy density and elastic energy density both rise as the unloading rate rises, while the dissipated energy density falls. The nonlinearity of the energy density versus relative cyclic number curves (Fig. 6a–c) is more pronounced as the unloading rate rises. Both percentages of elastic and dissipated energy densities can be divided into three stages, as shown in Fig. 6d. The percentage of elastic energy density increases quickly when the relative cyclic number is between 0.1 and 0.3, whereas the percentage of dissipated energy density is on the opposite. The percentages of elastic and dissipated energy densities both remain stable when the relative cyclic number is between 0.3 and 0.7. The percentages of elastic energy density decreases slightly and the percentages of dissipated energy density increases slightly when the relative cyclic number is between 0.7 and 1. In addition, the percentages of elastic and dissipated energy densities under different unloading rates change abnormally when the relative cyclic number is less than 0.2, which may be due to the difference of initial microcracks in the rock-like samples.

5. Damage evolution model

The aforementioned test results demonstrate that the strain and energy density of rock-like samples are significantly influenced by the unloading rate. The dissipated energy density is completely irrecoverable, in contrast to the elastic energy density, which can better reflect the damage caused by cyclic loading on the rock. As a result, many earlier researchers used the dissipated energy density to describe the degree of damage to rock-like samples (Li et al., 2022; Shirani Faradonbeh et al., 2022; Wang et al., 2022). The damage variable for the dissipated energy density can be expressed as follows in light of the cumulative variation properties of this quantity:

Please cite this article as: Liu Z et al., Deformation and damage properties of rock-like materials subjected to multi-level loading-unloading cycles, Journal of Rock Mechanics and Geotechnical Engineering, https://doi.org/10.1016/j.jrmge.2022.11.009

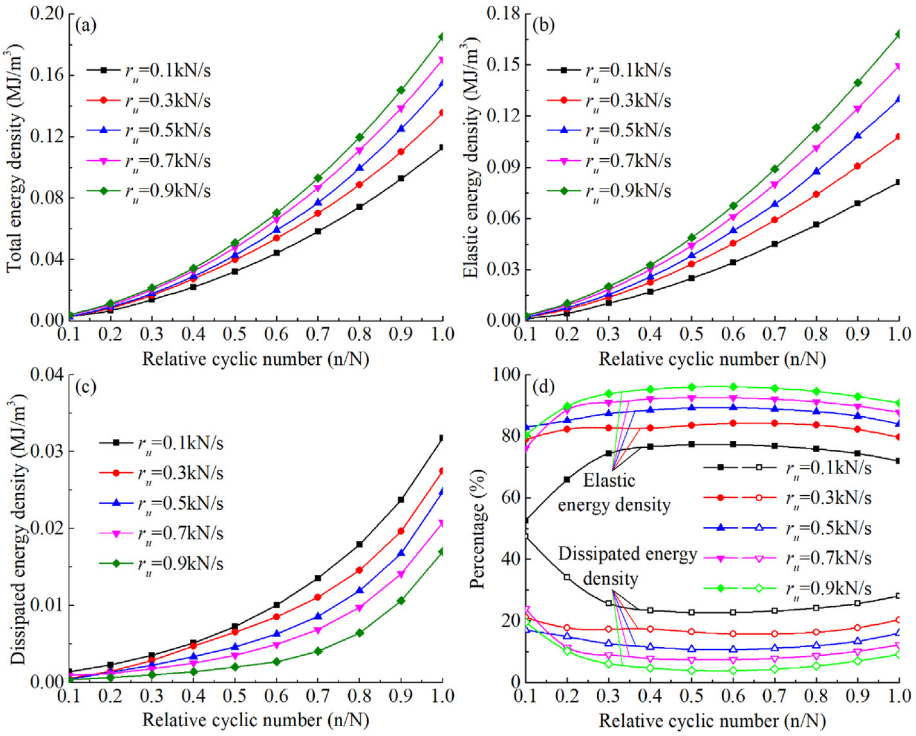

Fig. 6. Evolution laws of energy density of rock-like materials under different unloading rates: (a) The total energy density; (b) The elastic energy density; (c) The dissipated energy density; and (d) The percentages of elastic and dissipated energy densities in the total energy density.

$$D_e = \frac{\sum_{i=1}^{n} |u_p|_i}{\sum_{i=1}^{N} |u_p|_i} \tag{4}$$

where D_e represents the dissipated energy damage variable, i represents the ith cyclic loading-unloading, and n denotes the first n cycles of loading-unloading.

The dissipated energy damage variable of rock-like samples under various unloading rates was calculated in accordance with Eq. (4) and is plotted in Fig. 7. The variation of the dissipated energy damage variable under various unloading rates exhibits some similarity. In particular, the dissipated energy damage variable keeps growing as the relative cyclic number rises, and its variation can be divided into three stages: initial damage, stable damage, and accelerated damage. Additionally, for a given relative cyclic number, the dissipated energy damage variable is smaller under the higher unloading rate.

An inverted S-shaped nonlinear damage cumulative model has been proposed (Xiao et al., 2009), which can be used to calculate the cumulative damage of rock under multi-level cyclic loading-unloading, to characterize the evolution of damage accumulation of rock. The dissipated energy damage variable and relative cyclic number are related in the damage cumulative model, which can be expressed as

$$D_e = \alpha\left(\frac{\beta}{\beta - N_n} - 1\right)^{1/\gamma} \tag{5}$$

where α, β and γ are the fitting coefficients of dissipated energy damage variable related to the unloading rate; and N_n represents the relative cyclic number.

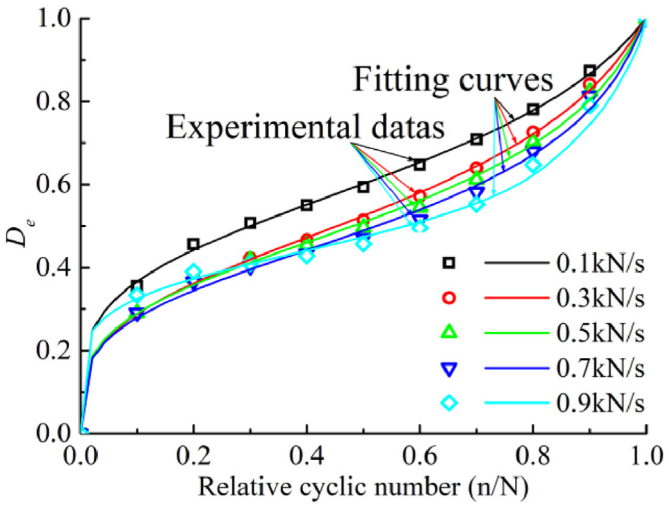

Fig. 7. The evolution of dissipated energy damage variable with relative cyclic number.

Table 1
The values of fitting coefficients related to the unloading rate.

r_u (kN/s)	α	β	γ	R^2
0.1	0.047	0.32	−0.054	0.9996
0.3	0.042	0.315	−0.051	0.9989
0.5	0.036	0.298	−0.044	0.9997
0.7	0.033	0.281	−0.032	0.9999
0.9	0.016	0.243	−0.012	0.9992

Eq. (5) was used to fit the dissipated energy damage variable. The fitting curves are displayed in Fig. 7. The values of fitting coefficients for different unloading rates are listed in Table 1. All the

Please cite this article as: Liu Z et al., Deformation and damage properties of rock-like materials subjected to multi-level loading-unloading cycles, Journal of Rock Mechanics and Geotechnical Engineering, https://doi.org/10.1016/j.jrmge.2022.11.009

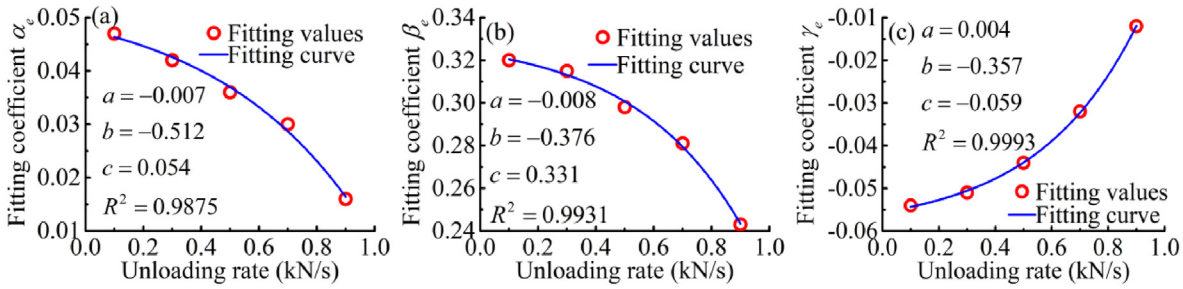

Fig. 8. The fitting results between the coefficients of the dissipated energy damage and unloading rate.

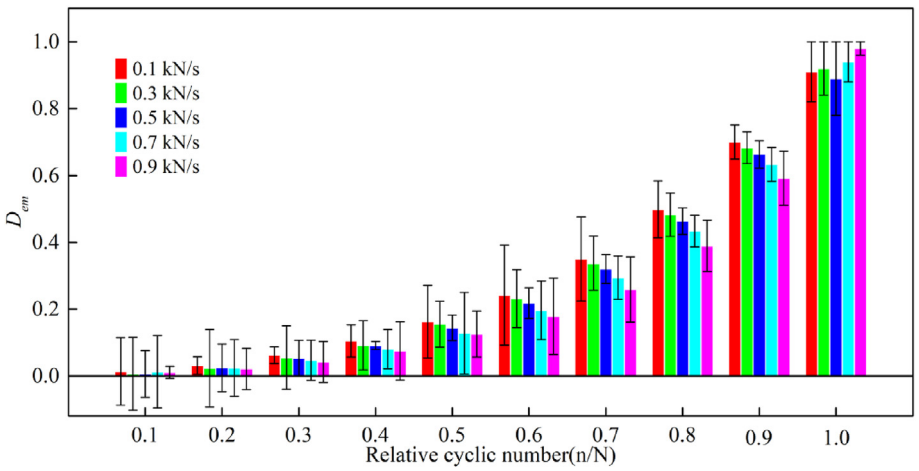

Fig. 9. The damage variables predicated by the dissipated energy damage model.

fitting curves have determination coefficients that are greater than 0.99. The fitting results show that Eq. (5) is appropriate to describe the variation of dissipated energy damage variable.

However, neither the physical significance of the parameters in Eq. (5) nor their relationship with the unloading rate is clear. Therefore, taking into account the impact of unloading rates, Eq. (5) cannot be used to predict the damage of rock-like materials in a direct manner. A damage model considering the unloading rate and relative cyclic number should be presented to address the aforementioned shortages. In order to determine the relationship between the unloading rate (r_u) and the coefficients in Eq. (5), fitting analysis was done based on the data in Table 1. Fig. 8 displays the fitting results, and the following equation is used to represent the fitting formula:

$$m = a\exp\left(-\frac{r_u}{b}\right) + c \tag{6}$$

where $m = \alpha$, β and γ.

The determination coefficients of all the fitting curves are above 0.98, verifying the reliability of the fitting formula.

By substituting Eq. (6) into Eq. (5), the dissipated energy damage model that takes into account the relative cyclic number and unloading rate can be expressed as follows:

$$D_{em} = \left(-0.007e^{r_u/0.512} + 0.054\right)\cdot \left(\frac{N_n}{-0.008e^{r_u/0.376} + 0.331 - N_n}\right)^{\frac{1}{0.004e^{r_u/0.357} - 0.059}} \tag{7}$$

Fig. 9 displays the dissipated energy damage variable (D_{em}) obtained by the proposed damage model. The dissipated energy damage variable obtained by Eq. (7) is represented by the histogram in Fig. 9, and the error bar represents the difference between D_{em} and the aforementioned experimental results (Fig. 7). Fig. 9 shows that D_{em} gradually increases with the increase of the relative cycle number. Except the relative cycle numbers of 0.1 and 1, D_{em} gradually decreases with the increase of unloading rate. Additionally, the average absolute error of energy dissipation damage predicted by the proposed damage model is 7.2%. As a result, the proposed damage model can accurately predict the energy damage of rock-like samples subjected to multi-level loading-unloading cycles.

6. Conclusions

In this paper, a series of uniaxial multi-level loading- unloading cycle experiments was performed to analyze the effect of unloading rate on the deformation characteristics and energy evolution laws of rock-like samples. A damage model was then put forth based on the energy lost by the rock-like samples. The main conclusions that can be drawn are as follows:

(1) The unloading rate and relative cyclic number clearly influence the strain characteristics of rock-like samples. In particular, as the relative cyclic number rises, the total strain and the reversible strain both grow linearly, whereas the irreversible strain first decreases quickly, then stabilizes, and finally increases slowly, clearly exhibiting nonlinear behavior. As the unloading rate increases, the total strain and reversible strain both increase, while the irreversible strain decreases.

Please cite this article as: Liu Z et al., Deformation and damage properties of rock-like materials subjected to multi-level loading-unloading cycles, Journal of Rock Mechanics and Geotechnical Engineering, https://doi.org/10.1016/j.jrmge.2022.11.009

(2) The unloading rate and relative cyclic number clearly affect the energy evolution of rock-like samples. The total energy density, elastic energy density, and dissipated energy density all exhibit a clear nonlinear increasing trend as the relative cyclic number rises. The total energy density and elastic energy density increase with increasing unloading rate, while the dissipated energy density decreases.
(3) Based on the correlation between the calculated dissipated energy damage variable and the relative cyclic number and unloading rate, a damage model was proposed. The dissipated energy damage variable of rock-like samples subjected to multi-level loading-unloading cycles can be accurately predicted by the proposed damage model, taking into account the effect of unloading rate, and the predicted results are in good agreement with the experimental findings.

This study assesses how the unloading rate affects the deformation and energy damage of rock-like material using a series of uniaxial multi-level loading-unloading cycle experiments. Then, a dissipated energy damage model considering the effect of unloading rate and relative cyclic number was proposed and verified, which will make it easier to foresee how the multi-level loading-unloading cycles affect the rock-like materials.

Declaration of competing interest

The authors declare that they have no known competing financial interests or personal relationships that could have appeared to influence the work reported in this paper.

Acknowledgements

We gratefully acknowledge the Water Conservancy Science and Technology Major Project of Hunan Province, China (Project XSKJ2019081-10), the China Scholarship Council (Grant No.202006370344), and the First-class Project Special Funding of Yellow River Laboratory, China (Grant No. YRL22YL07).

References

Bagde, M.N., Petroš, V., 2005. Fatigue properties of intact sandstone samples subjected to dynamic uniaxial cyclical loading. Int. J. Rock Mech. Min. Sci. 42 (2), 237–250.
Bagde, M.N., Petroš, V., 2009. Fatigue and dynamic energy behaviour of rock subjected to cyclical loading. Int. J. Rock Mech. Min. Sci. 46 (1), 200–209.
Chen, W.C., Li, S.D., Li, L., Shao, M.S., 2020. Strengthening effects of cyclic load on rock and concrete based on experimental study. Int. J. Rock Mech. Min. Sci. 135, 104479.
Chen, X., Huang, Y., Chen, C., Lu, J., Fan, X., 2017. Experimental study and analytical modeling on hysteresis behavior of plain concrete in uniaxial cyclic tension. Int. J. Fatig. 96, 261–269.
Chen, X., Tang, C., Kong, X., 2019. Study on progressive damage and failure of sandstone samples subjected to cyclic disturbance loads using a modified triaxial test system. KSCE J. Civ. Eng. 23 (5), 2371–2383.
Duan, M., Jiang, C., Gan, Q., Li, M., Peng, K., Zhang, W., 2020. Experimental investigation on the permeability, acoustic emission and energy dissipation of coal under tiered cyclic unloading. J. Nat. Gas Sci. Eng. 73, 103054.
Feng, P., Dai, F., Liu, Y., Xu, N., Du, H., 2019. Coupled effects of static-dynamic strain rates on the mechanical and fracturing behaviors of rock-like specimens containing two unparallel fissures. Eng. Fract. Mech. 207, 237–253.
Feng, P., Xu, Y., Dai, F., 2021. Effects of dynamic strain rate on the energy dissipation and fragment characteristics of cross-fissured rocks. Int. J. Rock Mech. Min. Sci. 138, 104600.
Fuenkajorn, K., Phueakphum, D., 2010. Effects of cyclic loading on mechanical properties of Maha Sarakham salt. Eng. Geol. 112 (1–4), 43–52.
Heap, M., Faulkner, D., 2008. Quantifying the evolution of static elastic properties as crystalline rock approaches failure. Int. J. Rock Mech. Min. Sci. 45 (4), 564–573.
Heap, M., Vinciguerra, S., Meredith, P., 2009. The evolution of elastic moduli with increasing crack damage during cyclic stressing of a basalt from Mt. Etna volcano. Tectonophysics 471 (1–2), 153–160.
Hu, B., Yang, S., Xu, P., Cheng, J., 2019. Cyclic loading–unloading creep behavior of composite layered specimens. Acta Geophys. 67 (2), 449–464.
Hu, J., Wen, G., Lin, Q., Cao, P., Li, S., 2020b. Mechanical properties and crack evolution of double-layer composite rock-like specimens with two parallel fissures under uniaxial compression. Theor. Appl. Fract. Mech. 108, 102610.
Hu, Q., Liu, L., Li, Q., Wu, Y., Wang, X., Jiang, Z., Yan, F., Xu, Y., Wu, X., 2020a. Experimental investigation on crack competitive extension during hydraulic fracturing in coal measures strata. Fuel 265, 117003.
Huang, D., Li, Y., 2014. Conversion of strain energy in triaxial unloading tests on marble. Int. J. Rock Mech. Min. Sci. 66, 160–168.
Jia, C., Xu, W., Wang, R., Wang, W., Zhang, J., Yu, J., 2018. Characterization of the deformation behavior of fine-grained sandstone by triaxial cyclic loading. Construct. Build. Mater. 162, 113–123.
Jiang, C., Duan, M., Yin, G., Wang, J., Lu, T., Xu, J., Zhang, D., Huang, G., 2017. Experimental study on seepage properties, AE characteristics and energy dissipation of coal under tiered cyclic loading. Eng. Geol. 221, 114–123.
Kendrick, J.E., Smith, R., Sammonds, P., Meredith, P.G., Dainty, M., Pallister, J.S., 2013. The influence of thermal and cyclic stressing on the strength of rocks from Mount St. Helens, Washington. Bull. Volcanol. 75 (7), 728.
Lavrov, A., 2001. Kaiser effect observation in brittle rock cyclically loaded with different loading rates. Mech. Mater. 33 (11), 669–677.
Li, C., Gao, C., Xie, H., Li, N., 2020. Experimental investigation of anisotropic fatigue characteristics of shale under uniaxial cyclic loading. Int. J. Rock Mech. Min. Sci. 130, 104314.
Li, T., Chen, G., Qin, Z., Li, Q., 2022. Analysis the characteristic of energy and damage of coal-rock composite structure under cycle loading. Geotech. Geol. Eng. 40 (2), 765–783.
Lin, Q., Cao, P., Cao, R., Lin, H., Meng, J., 2020. Mechanical behavior around double circular openings in a jointed rock mass under uniaxial compression. Arch. Civ. Mech. Eng. 20, 19.
Lin, Q., Cao, P., Liu, Y., Cao, R., Li, J., 2021a. Mechanical behaviour of a jointed rock mass with a circular hole under compression-shear loading: experimental and numerical studies. Theor. Appl. Fract. Mech. 114, 102998.
Lin, Q., Cao, P., Wen, G., Meng, J., Cao, R., Zhao, Z., 2021b. Crack coalescence in rock-like specimens with two dissimilar layers and pre-existing double parallel joints under uniaxial compression. Int. J. Rock Mech. Min. Sci. 139, 104621.
Liu, J., Xie, H., Hou, Z., Yang, C., Chen, L., 2014. Damage evolution of rock salt under cyclic loading in unixial tests. Acta Geotech 9 (1), 153–160.
Liu, Z., Cao, P., Li, K., Wang, F., Dong, T., Liu, J., 2022. Fracture analysis of central-flawed rock-like specimens under the influence of coplanar or non-coplanar edge flaws. Bull. Eng. Geol. Environ. 81, 61.
Ma, L., Liu, X., Wang, M., Xu, H., Hua, R., Fan, P., Jiang, S., Wang, G., Yi, Q., 2013. Experimental investigation of the mechanical properties of rock salt under triaxial cyclic loading. Int. J. Rock Mech. Min. Sci. 62, 34–41.
Meng, G., Liu, Z., Cao, P., Zhang, Z., Fan, Z., Lin, H., Deng, H., 2022. An initial damage model of rock materials under uniaxial compression considering loading rates. Materials 15 (16), 5589.
Meng, Q., Zhang, M., Han, L., Pu, H., Nie, T., 2016. Effects of acoustic emission and energy evolution of rock specimens under the uniaxial cyclic loading and unloading compression. Rock Mech. Rock Eng. 49 (10), 3873–3886.
Meng, Q., Zhang, M., Zhang, Z., Han, L., Pu, H., 2019. Research on non-linear characteristics of rock energy evolution under uniaxial cyclic loading and unloading conditions. Environ. Earth Sci. 78, 650.
Momeni, A., Karakus, M., Khanlari, G., Heidari, M., 2015. Effects of cyclic loading on the mechanical properties of a granite. Int. J. Rock Mech. Min. Sci. 77, 89–96.
Peng, K., Wang, Y., Zou, Q., Liu, Z., Mou, J., 2019. Effect of crack angles on energy characteristics of sandstones under a complex stress path. Eng. Fract. Mech. 218, 106577.
Peng, K., Zhou, J., Zou, Q., Song, X., 2020. Effect of loading frequency on the deformation behaviours of sandstones subjected to cyclic loads and its underlying mechanism. Int. J. Fatig. 131, 105349.
Pouya, A., Zhu, C., Arson, C., 2016. Micro–macro approach of salt viscous fatigue under cyclic loading. Mech. Mater. 93, 13–31.
Shirani Faradonbeh, R., Taheri, A., Karakus, M., 2021. Post-peak behaviour of rocks under cyclic loading using a double-criteria damage-controlled test method. Bull. Eng. Geol. Environ. 80 (2), 1713–1727.
Shirani Faradonbeh, R., Taheri, A., Karakus, M., 2022. Fatigue failure characteristics of sandstone under different confining pressures. Rock Mech. Rock Eng. 55 (3), 1227–1252.
Taheri, A., Yfantidis, N., Olivares, C., Connelly, B., Bastian, T., 2016. Experimental study on degradation of mechanical properties of sandstone under different cyclic loadings. Geotech. Test J. 39 (4), 673–687.
Vaneghi, R.G., Ferdosi, B., Okoth, A.D., Kuek, B., 2018. Strength degradation of sandstone and granodiorite under uniaxial cyclic loading. J. Rock Mech. Geotech. Eng. 10 (1), 117–126.
Vaneghi, R.G., Thoeni, K., Dyskin, A.V., Sharifzadeh, M., Sarmadivaleh, M., 2020b. Fatigue damage response of typical crystalline and granular rocks to uniaxial cyclic compression. Int. J. Fatig. 138, 105667.
Vaneghi, R.G., Thoeni, K., Dyskin, A.V., Sharifzadeh, M., Sarmadivaleh, M., 2020a. Strength and damage response of sandstone and granodiorite under different loading conditions of multistage uniaxial cyclic compression. Int. J. GeoMech. 20 (9), 04020159.
Wang, C., He, B., Hou, X., Li, J., Liu, L., 2020. Stress–energy mechanism for rock failure evolution based on damage mechanics in hard rock. Rock Mech. Rock Eng. 53 (3), 1021–1037.

Please cite this article as: Liu Z et al., Deformation and damage properties of rock-like materials subjected to multi-level loading-unloading cycles, Journal of Rock Mechanics and Geotechnical Engineering, https://doi.org/10.1016/j.jrmge.2022.11.009

Wang, W., Wang, Y., Chai, B., Du, J., Xing, L., Xia, Z., 2022. An energy-based method to determine rock brittleness by considering rock damage. Rock Mech. Rock Eng. 55 (3), 1585–1597.

Wang, Y., Gao, S., Li, C., Han, J., 2021. Energy dissipation and damage evolution for dynamic fracture of marble subjected to freeze-thaw and multiple level compressive fatigue loading. Int. J. Fatig. 142, 105927.

Xiao, J., Ding, D., Xu, G., Jiang, F., 2009. Inverted S-shaped model for nonlinear fatigue damage of rock. Int. J. Rock Mech. Min. Sci. 46 (3), 643–648.

Xiao, J., Ding, D., Xu, G., Jiang, F., 2008. Waveform effect on quasi-dynamic loading condition and the mechanical properties of brittle materials. Int. J. Rock Mech. Min. Sci. 45 (4), 621–626.

Yang, S., Hu, B., 2018. Creep and long-term permeability of a red sandstone subjected to cyclic loading after thermal treatments. Rock Mech. Rock Eng. 51 (10), 2981–3004.

Zhang, P., Yuan, P., Guan, J., Yao, X., Li, L., 2021. Statistical analysis of three-point-bending fracture failure of mortar. Construct. Build. Mater. 300, 123883.

Zhang, M., Dou, L., Konietzky, H., Song, Z., Huang, S., 2020. Cyclic fatigue characteristics of strong burst-prone coal: experimental insights from energy dissipation, hysteresis and micro-seismicity. Int. J. Fatig. 133, 105429.

Zhang, M., Meng, Q., Liu, S., Qian, D., Zhang, N., 2018. Impacts of cyclic loading and unloading rates on acoustic emission evolution and felicity effect of instable rock mass. Adv. Mater. Sci. Eng. 2018, 8365396.

Zhou, C., Xie, H., Zhu, J., Wang, Z., Li, C., Wang, F., 2022. Mechanical and fracture behaviors of brittle material with a circular inclusion: Insight from infilling composition. Rock Mech. Rock Eng. 55, 3331–3352.

Zhou, Y., Sheng, Q., Li, N., Fu, X., 2020. Numerical analysis of the mechanical properties of rock materials under tiered and multi-level cyclic load regimes. Soil Dynam. Earthq. Eng. 135, 106186.

Zhu, Y., Yu, J., Zhou, X., Yang, Z., Tang, X., Liu, X., 2021. Uniaxial stress relaxation behavior of marble after cyclic disturbance loads. Mech. Time-Dependent Mater. 25 (4), 513–537.

Fei Wang is presently working as a assistant research fellow in Yellow River Laboratory, Zhengzhou University (ZZU), China. He obtained his MSc and PhD degrees from Central South University, China and completed his post-doctoral program in Shenzhen University, China in 2021. His research interests include rock fracture mechanics and failure mechanism of underground engineering. He has vast practical experience in laboratory and field testing of rock mechanics. He has published more than 20 journal or conference papers indexed by SCI/EI.

Please cite this article as: Liu Z et al., Deformation and damage properties of rock-like materials subjected to multi-level loading-unloading cycles, Journal of Rock Mechanics and Geotechnical Engineering, https://doi.org/10.1016/j.jrmge.2022.11.009